Feature Optics and the Critical Planes of the Grating

Paul Mirsky
paulmirsky633@gmail.com

September 8, 2019

Abstract

Feature optics (FO) was recently proposed as a new tool which models the beam and the grating as combinations of simple elements called *features*. This work applies FO to the many patterns formed by the light from a grating as it propagates into the far field, passing through various planes. We find that the entire process can be expressed naturally and beautifully in terms of FO.

1 Introduction

Feature optics (FO) is a new framework for describing diffraction and interference, first introduced in reference 1. That work established the principles of FO and applied them to the grating in the 2f system, in which a lens is used to effect a Fourier Transform (FT) on an input function. Please note, this work assumes that the reader is already familiar with FO from reference 1.

The scope of the previous work was limited to the input and output planes of the system, which lie at the front and rear focal planes of the lens, respectively. This work extends that scope by describing the many intermediate planes and stages in between the input and output. This gives a much more complete picture of how light transforms as it propagates.

The diffraction grating is one of the most basic optical devices. The most typical type consists of a plane wave source filtered by an opaque screen with a periodic array of identical apertures. Its essential principle is that when a periodic pattern of coherent light propagates into the far field, it transforms into a *different* periodic pattern. By far its most common practical application is to separate light into its component wavelengths; however, we will consider only monochromatic light.

At present, FO is a tool for *description* rather than explanation. In other words, it is not grounded in any theory and it does not give an account of how or why it works. Rather, it is simply a system for describing the structure of certain patterns of light. Its value lies in its uncanny aptness for describing those patterns, and because it casts the FT such a simple form. Many fundamental questions about FO remain unanswered, but invite deeper investigation.

This work will begin with a short overview of the *critical planes* of the propagating grating. Next, we will step through the stages of propagation, treating each one in detail using the methods of FO. Finally we discuss and summarize our results, which includes comparing the FO analysis against the conventional wave-optics description.

Companion code written in Matlab is available on Github[2]. It calculates the patterns and positions of many planes in the propagating grating using FO, and recreates many of the diagrams in this work.

2 Overview of critical planes and stages

Earlier work in FO has dealt only with two planes: the input and output planes of a 2f system, where the curvature of the wavefront is flat. In this work we look at other, intermediate planes. While there exist an infinite number of these, we will describe only certain *critical planes*. Many other planes can be understood approximately by interpolating between two critical planes, while yet other planes are not well-described by FO and will be left out of the analysis.

An overview of the critical planes appears in figure 2.1. This figure is meant only as a qualitative schematic, *not* a precise drawing. It is not accurately scaled, and relative sizes appear wildly distorted.

figure 2.1, Schematic overview of critical planes

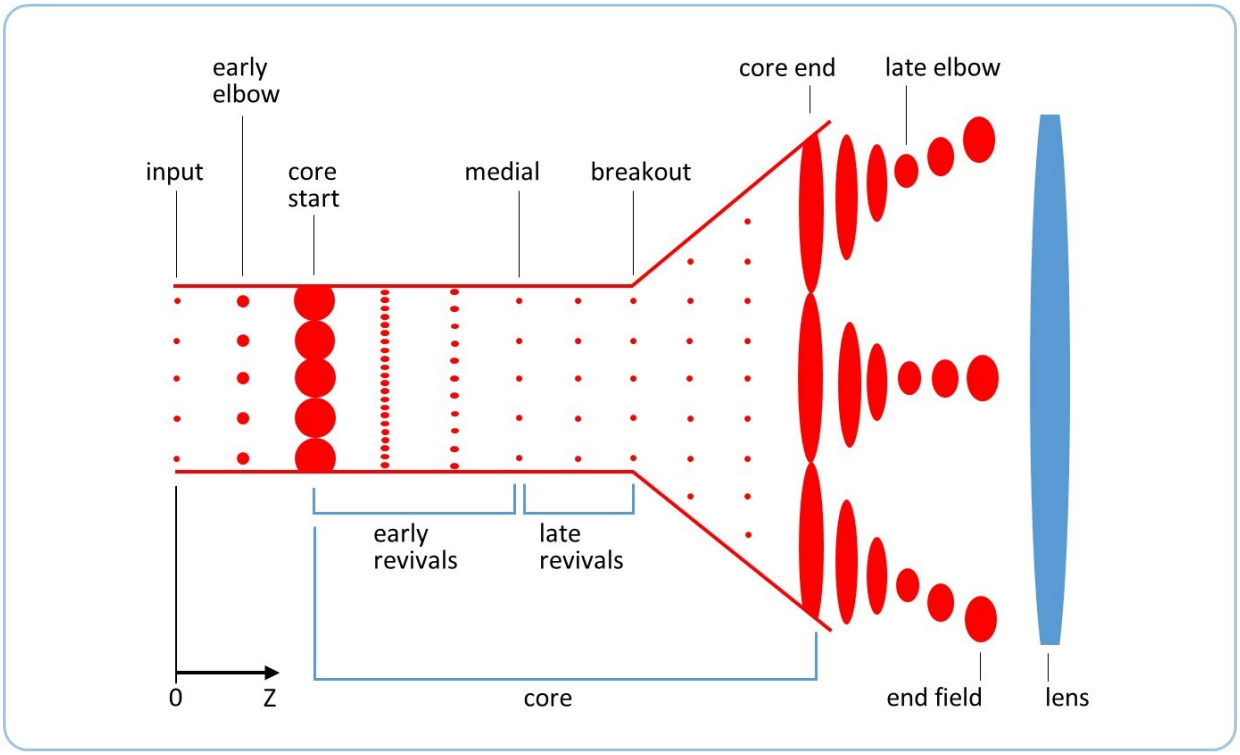

A grating pattern is placed at the *input plane* at Z = 0. The grating pattern is structured as a nested chain[1] of 4 features of sizes A, B, C, and D. It may also be thought of as a periodic array of identical instances of a small beam of diameter A, which we call the *early beam*; the overall extent of the array acts like a large beam of diameter ABC, which we call the *late beam*. Note that all sizes and distances in this work are given in units of wavelengths.

The early beam instances propagate forward as if they were independent beams, at first becoming only slightly wider. The plane $Z = A^2$ is the *early elbow*, also called the Rayleigh range of the early beam.

In the next stage, the beam instances grow much wider while the period remains constant. The separate instances eventually begin to overlap one another at the *core start* plane at $Z = A^2B$.

The next several stages are collectively called the *core*; in this region, complex periodic patterns fluctuate rapidly with change in Z. Certain significant planes are called the *early revivals.* The last of these is the *medial* at $Z = A^2B^2$, which appears as a staggered replica of the input pattern.

As the core continues there appear additional replicas called the *late revivals*, which repeat at regular intervals until the *breakout* plane at $Z = A^2B^2(C/B)$.

Up to the breakout, the overall width of the pattern remains nearly constant as the inner details evolve. After breakout, the overall width increases. At the same time, the bright areas within the pattern expand to fill the interstitial space, eventually forming an even distribution at the *core end* at $Z = A^2B^2C$.

The large area at the core end then divides into multiple instances of the late beam, which remain at a constant area but grow further apart from one another until the *late elbow* at $Z = A^2B^2C^2$.

After the late elbow the pattern continues to grow with propagation. However, its shape no longer changes – rather, the entire pattern is simply magnified uniformly. In principle, this can continue indefinitely; however, in a 2f system the light is eventually captured by a lens at the *end field* plane at $Z = A^2B^2C^2Y$, where Y is some magnification factor.

The lens changes the curvature of the light, but does not change its distribution in space. On the far side of the lens, the distribution remains constant as it propagates, eventually reaching the output at the rear focal plane. This completes the Fourier transform of the input pattern.

3 The input

Now we begin our detailed analysis of the propagating grating using FO. The grating begins with a flat wavefront at the input plane. The distribution of amplitude is uniform at all bright points,

and all phase factors are zero. The shape of the bright and dark pattern is described by a nested chain of four features (bright, dark, bright, dark) as shown in the *feature diagram* figure 3.1a. Each feature has a size, which may be any integer. We label the sizes A, B, C, and D, starting with the lowest nesting rank and proceeding to the highest.

figure 3.1, Feature and spatial diagrams of input pattern

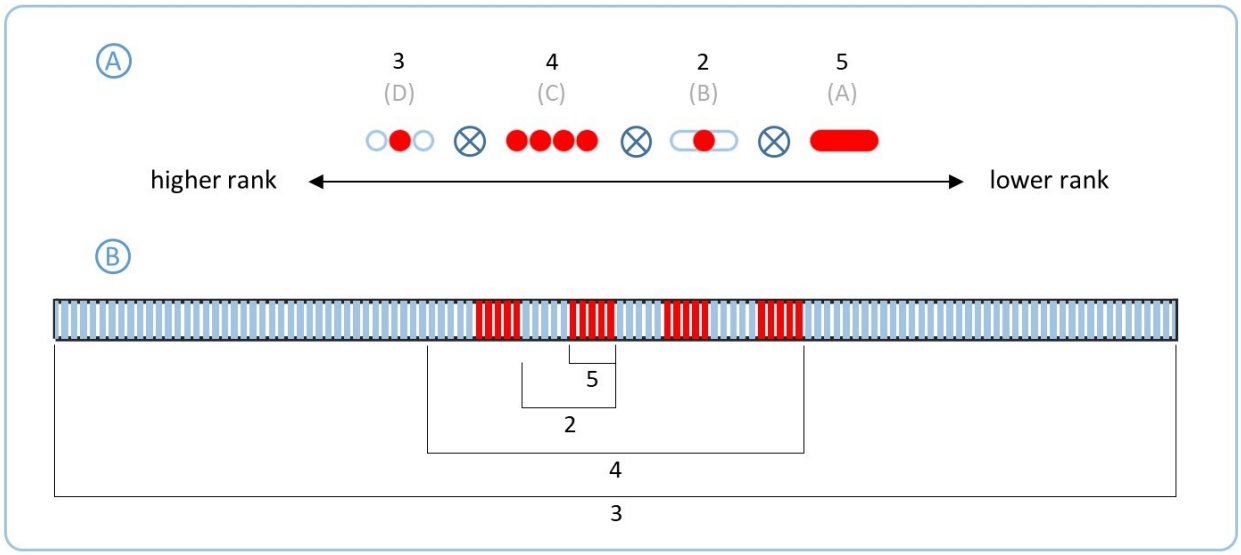

We now introduce some alternative conventions for feature diagrams. In reference 1, we always depicted each feature as a series of discrete patches, such as features C and D (sizes 4 and 3) in figure 3.1a. To keep the diagram small, we may sometimes draw a feature as a continuous bar, indicating its size with a label (the length of the bar carries no meaning), such as features A and B (sizes 5 and 2).

The corresponding spatial diagram in figure 3.1b shows how the pattern actually looks in physical space. Please note that while this spatial diagram shows the *entire* space under consideration, this work may also use 'zoomed' spatial diagrams that show only the relevant part of the space.

As we step through each stage of the propagation, we will draw such spatial and feature diagrams. To keep the illustrations manageably small, we will frequently change the values of A, B, C, and D from one stage to another; however, these example values will always remain constant within any one stage. Note that this is unlike a real grating, in which the parameters always remain constant during the entire propagation history.

This work considers only the case in which C > B, which we call the *late-breaking grating*. In this case, late revivals occur and a breakout plane occurs after the medial. This condition holds for a typical diffraction grating, but is broken for some possible gratings including the classic double-slit experiment (C = 2, B = large).

In order to study the simplest-possible case, we require that all but a negligible amount of the Fourier transform occur *before* the lens. This is equivalent to requiring that D > ABC, or equivalently that D = ABCY where Y is some end-field magnification factor. This is an impractical case to realize experimentally, because it would typically require a giant lens many meters across, and a laboratory bench many tens or even hundreds of meters in length. However, it is a very convenient case to study because it is equivalent to a freely-expanding beam (i.e. with no lens).

4 The early elbow

The first stage is somewhat trivial – it appears that no change is occurring at all. Actually, the most interesting aspect of this stage will become clearest in hindsight, when we summarize the overall trends.

The plane of the early elbow is only A^2 waves from the input. The spatial diagram in figure 4.1 shows that the pattern of light does not evolve appreciably over this short distance; the small change that does in fact occur will be discussed at the end of the next section. Note that this diagram is zoomed, showing only about 1/36 (1/D) of the total space; the remainder is dark area.

figure 4.1, Spatial diagram of stage approaching the early elbow

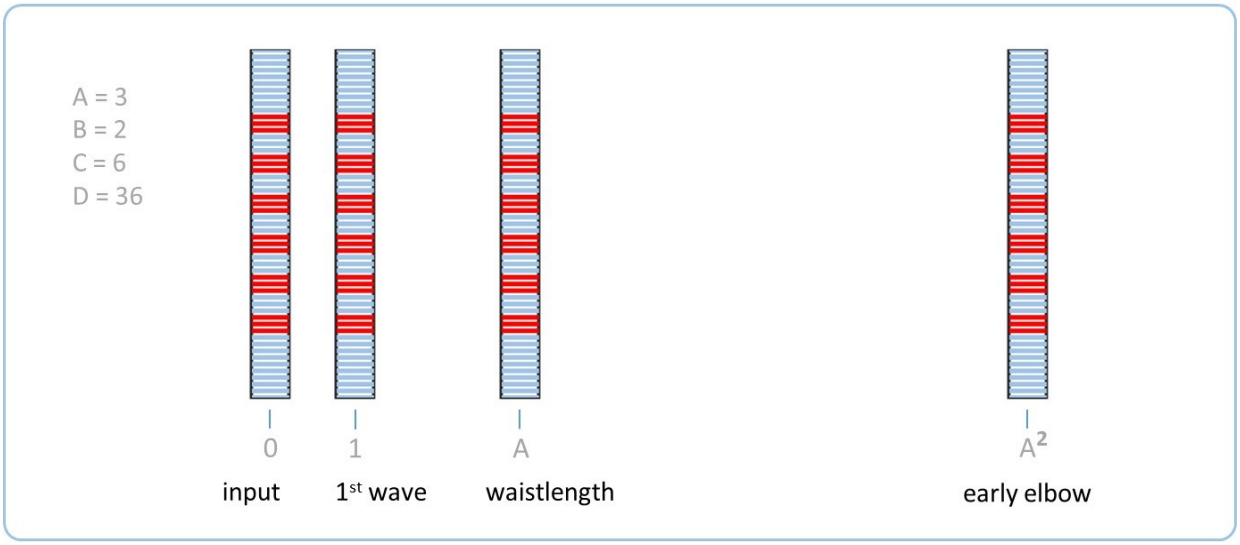

See companion code in earlyElbow.m

The feature diagram in figure 4.2 shows a similarly uneventful progression:

figure 4.2, Feature diagram of stage approaching the early elbow

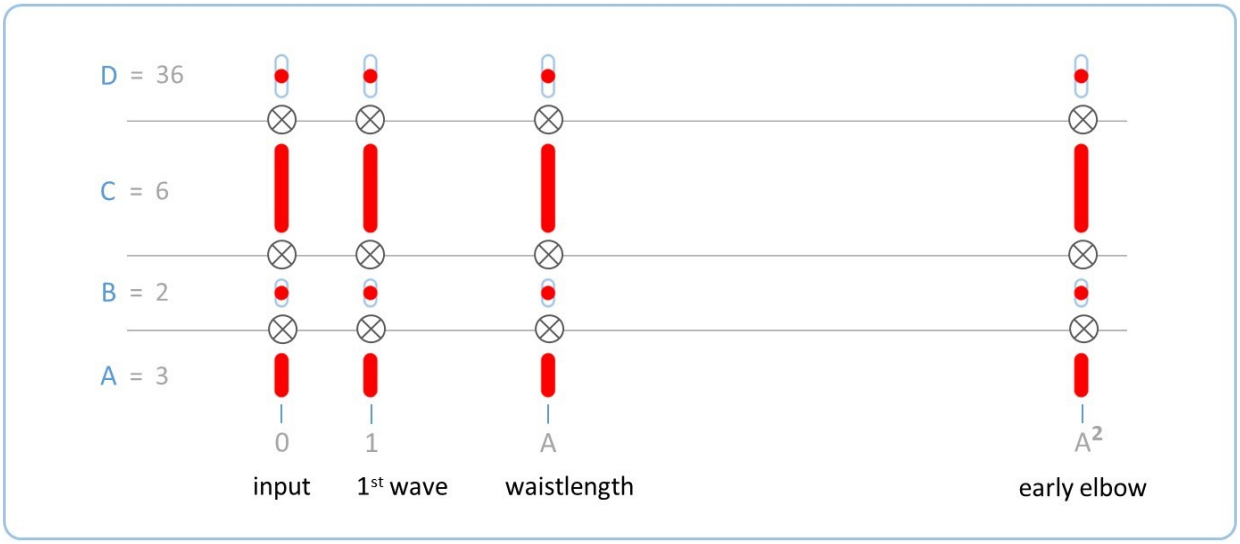

5 The core start

After the early elbow, the early beam instances begin to expand in width, as shown in the spatial diagram in figure 5.1. For any point between the early elbow and the core start, the beam width is linearly proportional to Z; its divergence is 1/A, which will eventually persist after the core end as the divergence of the outermost extent of the pattern.

figure 5.1, Spatial diagram of stage approaching the core start

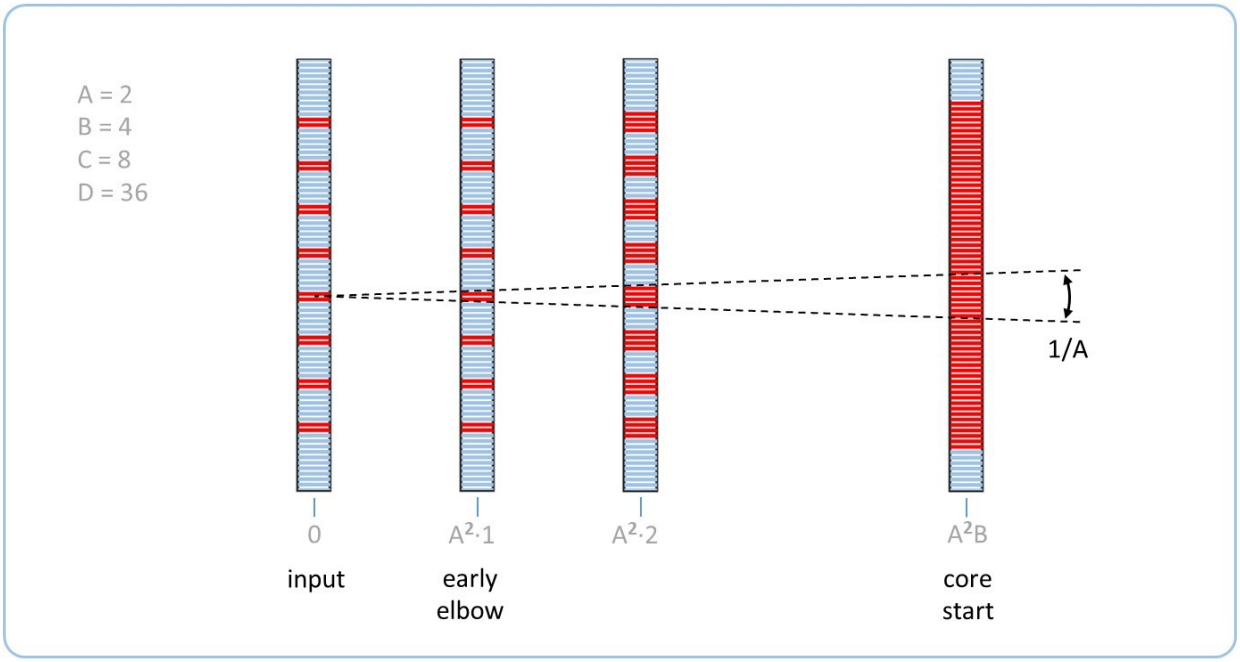

See companion code in coreStart.m

The core start occurs when the early beam grows to the width of the period, eliminating the dark space in between the individual instances. The period in this case is AB, and the beam divergence 1/A; thus, the core start occurs at distance $Z = A^2B$.

At this point we can compare FO against the Gaussian beam model, which matches experiment very closely. As figure 5.2 shows, the Gaussian beam propagates with minimal expansion for a short distance, reaching sqrt(2) times its starting diameter at the Rayleigh range. The angle then gets steeper, asymptotically approaching the shape of a cone. In contrast, the FO model divides the beam into two discrete regions: a straight region with zero expansion from the waist to the elbow, and a cone-like region which begins abruptly at the elbow, giving the elbow its name. The two models converge at the waist and in the far field, and the greatest discrepancy occurs at the elbow.

figure 5.2, Gaussian beam vs FO beam

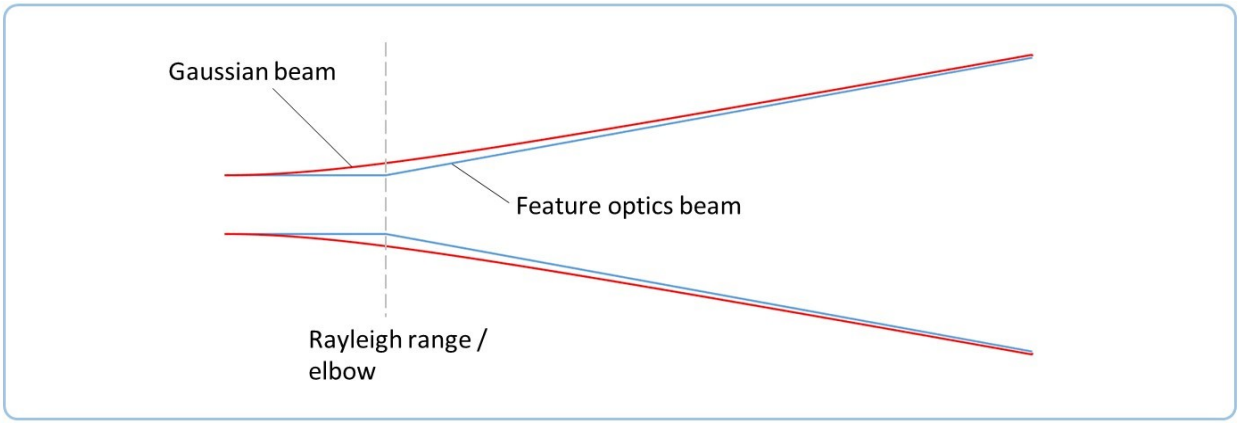

The feature diagram is drawn in figure 5.3. It shows that the changes leading to the core start can be expressed as a gradual change of feature B from dark to bright. We can factor feature B into two sub-features: a bright feature B_1 and a dark feature B_2, whose sizes change but always multiply to B. At the early elbow, $B_1 = 1$ and $B_2 = 4$; here, the division into two features is trivial, since a feature of size 1 makes no physical difference. As the light propagates, the bright feature B_1 grows in linear proportion to Z, while the dark feature B_2 shrinks in proportion to 1/Z. By the core start, B_1 has grown to the full value of B (4) while B_2 is trivial (1).

figure 5.3, Feature diagram of stage approaching the core start

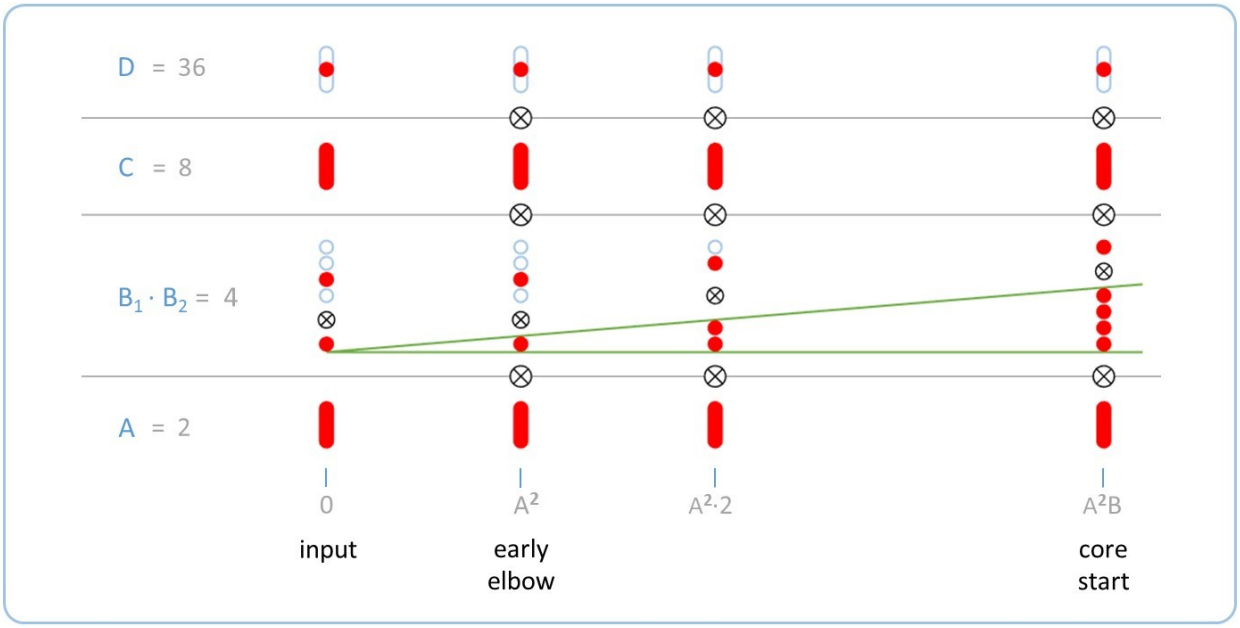

Note that in order to keep the diagrams simple, we draw only the planes in which both B_1 and B_2 are integers. However, the structure of other planes is clear by simple interpolation.

While the spatial and feature diagrams show essentially the same thing, the spatial diagram tends to suggest that the dark space between beams is a passive vacuum, into which the bright beams actively expand. In contrast, the feature diagram gives roughly equal emphasis to both bright and dark features.

6 Early revivals and the medial

In the foregoing stage, the changes in shape were gradual and continuous, so that while we showed only a small number of planes, it was clear that any other plane could easily be understood by interpolation. The present stage is different, because while we will describe a small number of critical planes showing a clear trend, the planes in between those do not follow the trend at all – instead, they vacillate rapidly and drastically. These intermediate planes are not included in this analysis.

The spatial diagram in figure 6.1 shows the somewhat counter-intuitive trend. Between the input and the core start, dark space between beams gradually dwindled away. In the current stage it reappears, producing a curious effect immediately after the core start, in which one large contiguous bright area appears to suddenly 'fragment' into many discrete smaller bright areas with dark areas in between. The dark space grows wider in proportion to Z, continuing until the *medial* plane at $Z = A^2B^2$, where the pattern appears as a replica of the input pattern, staggered laterally by half a period.

figure 6.1, Spatial diagram of early revivals in stage approaching the medial

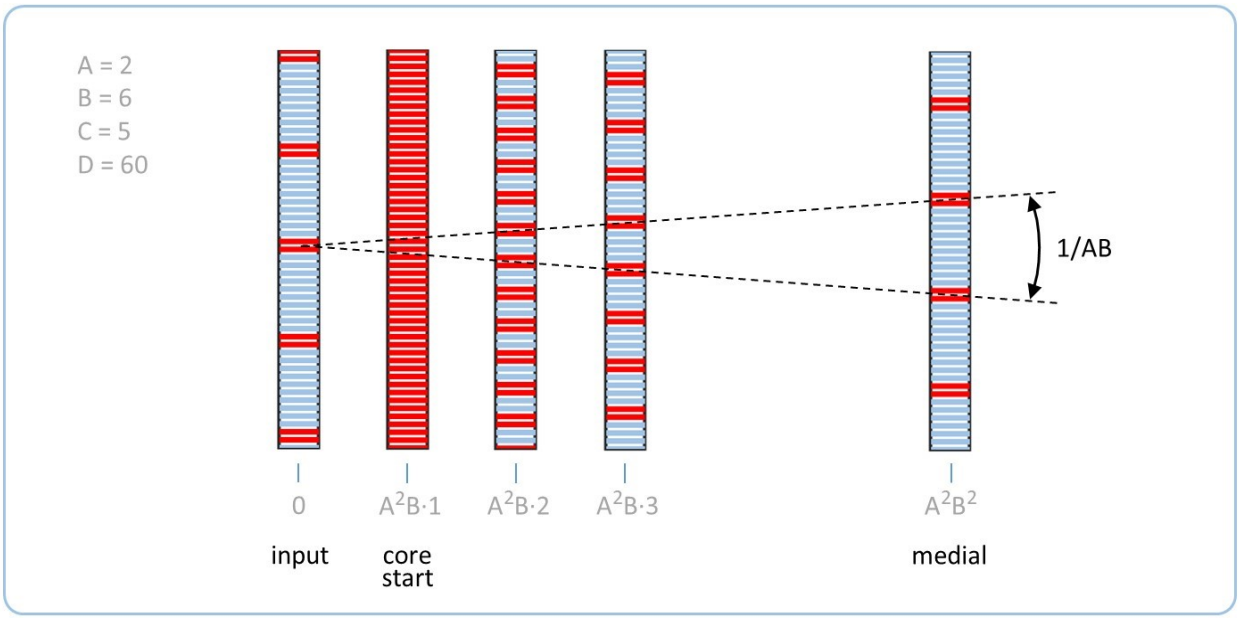

See companion code in medial.m

The trend is manifest only in certain critical planes called the *early revivals*, some of which are shown in the figure; related planes called *late revivals* will occur in the subsequent stage. These partially coincide with what are conventionally called *Talbot images*; however, these are not simply two different terms for the same thing – rather, they belong to two different schemes for classifying the planes. We will clarify these distinctions in section 12.2.

While the bright areas grow further apart from one another, the bright areas themselves remain at constant size A, the starting area of the early beam. Additionally, the outer limits of the pattern remain constant. With both of these sizes fixed, the *number* of repeated periods shrinks in inverse proportion to the growing dark space.

The bright areas appear to diverge from one another at a separation angle of 1/AB. Curiously, this same separation angle will appear later on as the angle between orders (instances of the late beam) in the far field. It is tempting to view each bright area as a far-field order in the process of formation; however, this is not quite correct because the number of bright areas changes, and it is not possible to track the identity of an individual bright area from one plane to another.

The locations of the early-revival planes make more sense in the context of the feature diagram, see figure 6.2. As in the stage leading up to the core start, feature B is factored into two sub-features B_1 and B_2, with B_1 ranked lower in the feature chain. However, in this instance B_1 is a dark feature and B_2 is a bright feature, which is the reverse of the case in the previous stage.

figure 6.2, Feature diagram of early revivals in stage approaching the medial

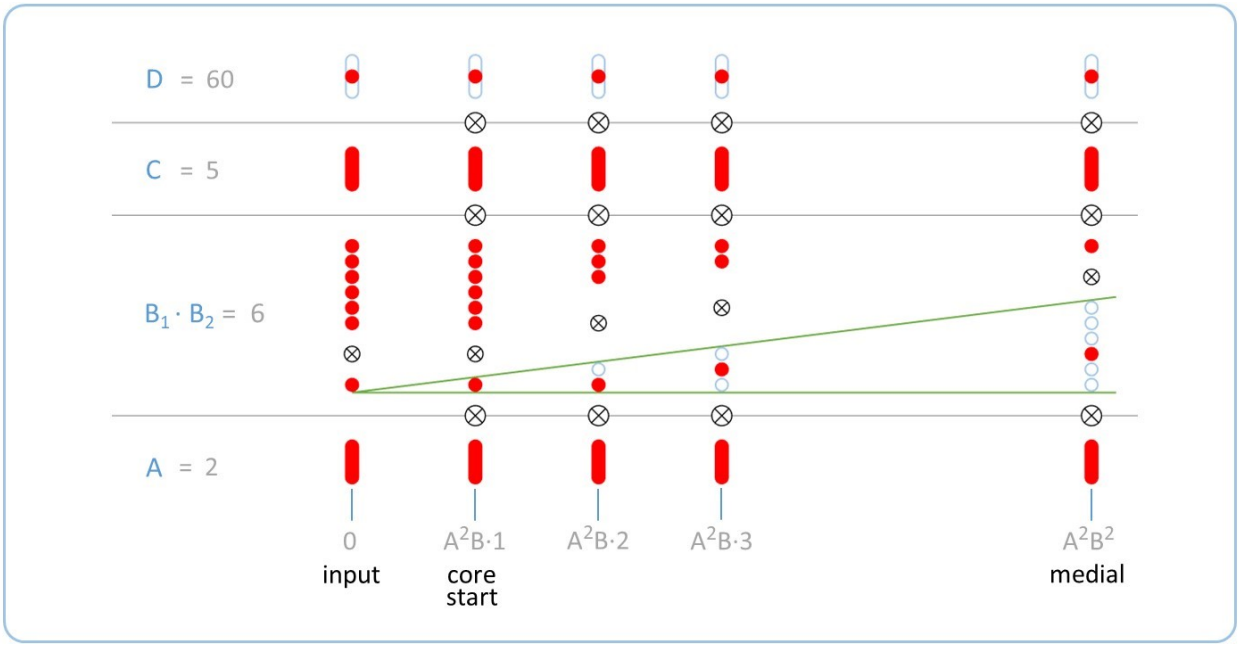

The early revivals are governed by the bright feature B_2. As B_2 decreases from B to 1, an early revival occurs at each plane where B_2 is a whole number of patches. Note that these planes are *not* spaced evenly in Z; instead, they are mostly bunched close to the core start, occurring at planes where

$$Z = \frac{Z_{medial}}{n}, \quad n \in \{ 1, 2, 3 \ldots B \}$$

Note that figure 6.2 does *not* show all of the early revivals, because it shows only planes in which both B_1 and B_2 are whole numbers.

7 Late revivals and breakout

In discussing the stage following the medial, we make the assumption that C > B, or equivalently that the ratio C/B is greater than 1. This ratio determines the length of this stage. It is certainly possible for gratings to exist in which this condition does not hold, but they have not yet been studied.

The present stage extends from the medial to the *breakout* plane. To appreciate the significance of breakout, refer either to figure 2.1 in the overview above or to figure 8.1 in the following section. The present spatial diagram in figure 7.1 appears remarkably dull – it shows the same pattern, repeated C/B times. However, this does not describe a static pattern remaining constant over time; rather, it describes the *late revivals*, which are recurring instances of the

input pattern separated by regions of fluctuation. (A later section will discuss the relationship between the late revivals and Talbot images.)

figure 7.1, Spatial diagram of late revivals in stage approaching breakout

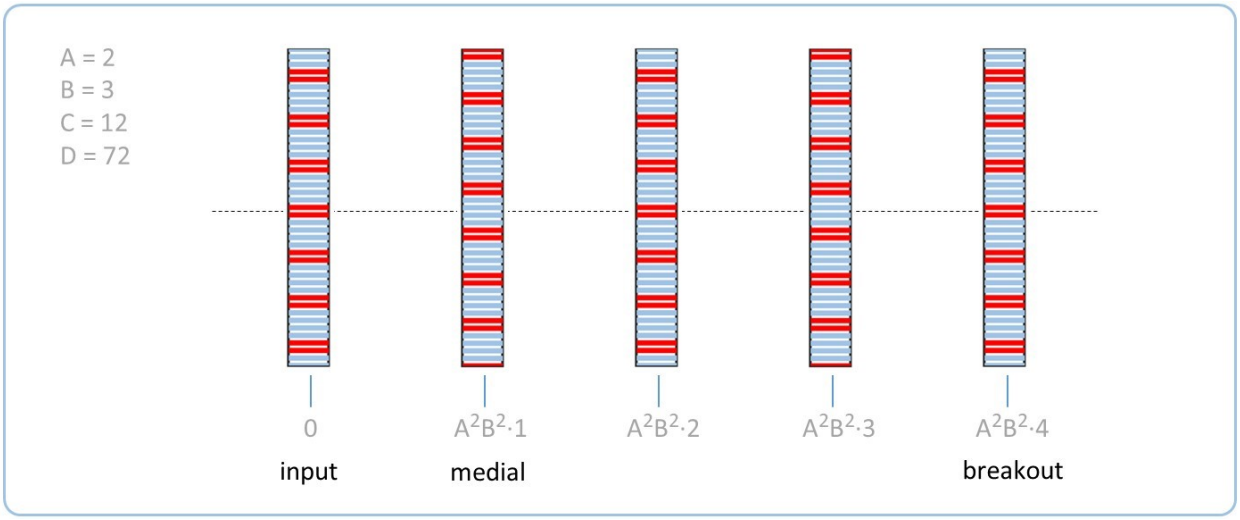

Recall that the grating began as an input pattern and changed shape as it propagated through several stages before reaching the medial, where the original input pattern formed once again. Each step from one late revival to the next is essentially a repetition of this entire sequence. The diagrams do not show this cyclic fluctuation – as with the early revivals, we account for certain planes but not others.

The feature diagram, like the corresponding spatial diagram, is simply a repetition of the input pattern (see figure 7.2).

figure 7.2, Feature diagram of late revivals in stage approaching breakout

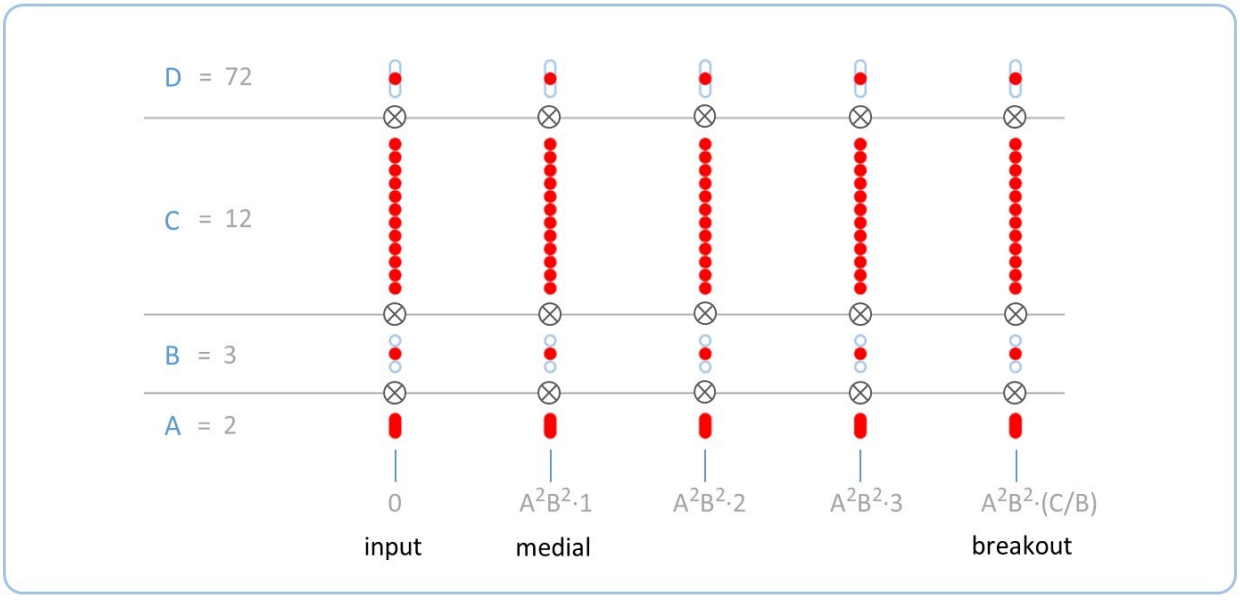

8 The core end

A grating pattern is typically formed by illuminating a grating screen with a wide collimated source, whose width sets the overall extent of the pattern. From the start of propagation through breakout, the outer extent of the pattern propagates like a collimated beam, without widening. After breakout, the single large beam grows to become B distinct beams, each one as wide as the original, as drawn in figure 8.1. Some authors use the term *walkoff* [3] rather than breakout.

figure 8.1, Spatial diagram of stage approaching the core end

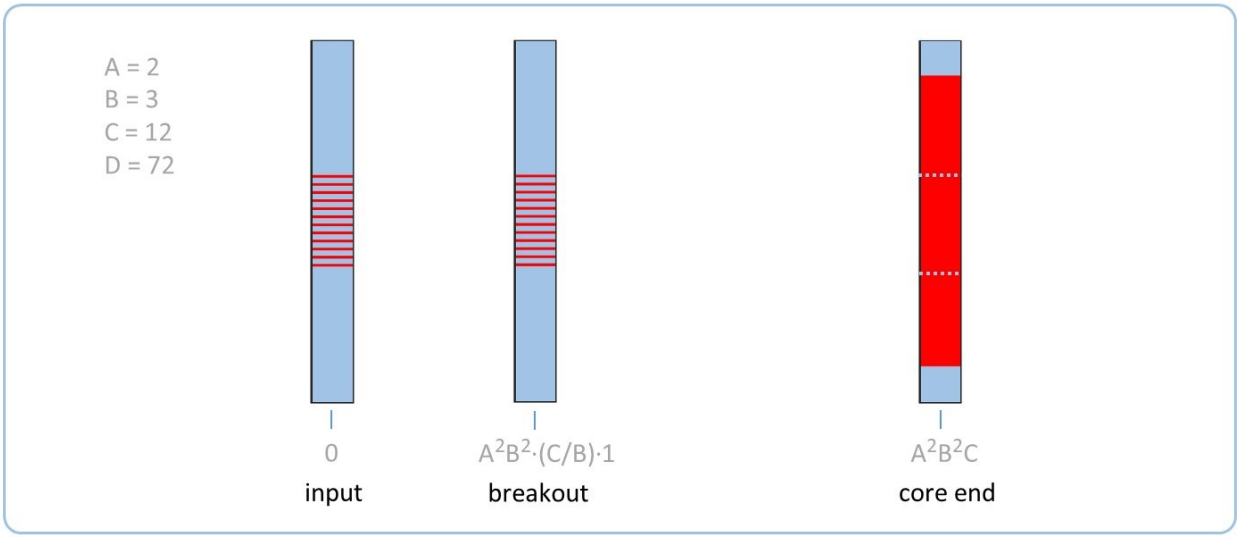

See companion code in coreEnd.m

The bright areas inside the pattern also widen simultaneously with the increase in overall width. As they do, the late revivals gradually degrade[3,4]. The cyclic fluctuation from one revival to the next also stops, and is replaced by a stable pattern which changes only gradually with distance.

These trends terminate at the *core end*, which is analogous to the core start but occurs in reverse. At the core start, the individual instances of the small early beam expand to the point of overlap; at the core end, instances of the late beam emerge from overlap.

The feature diagram in figure 8.2 shows that the outer extent appears to widen in tandem with the revivals, which is less apparent when visualized in a spatial diagram.

figure 8.2, Feature diagram of stage approaching the core end

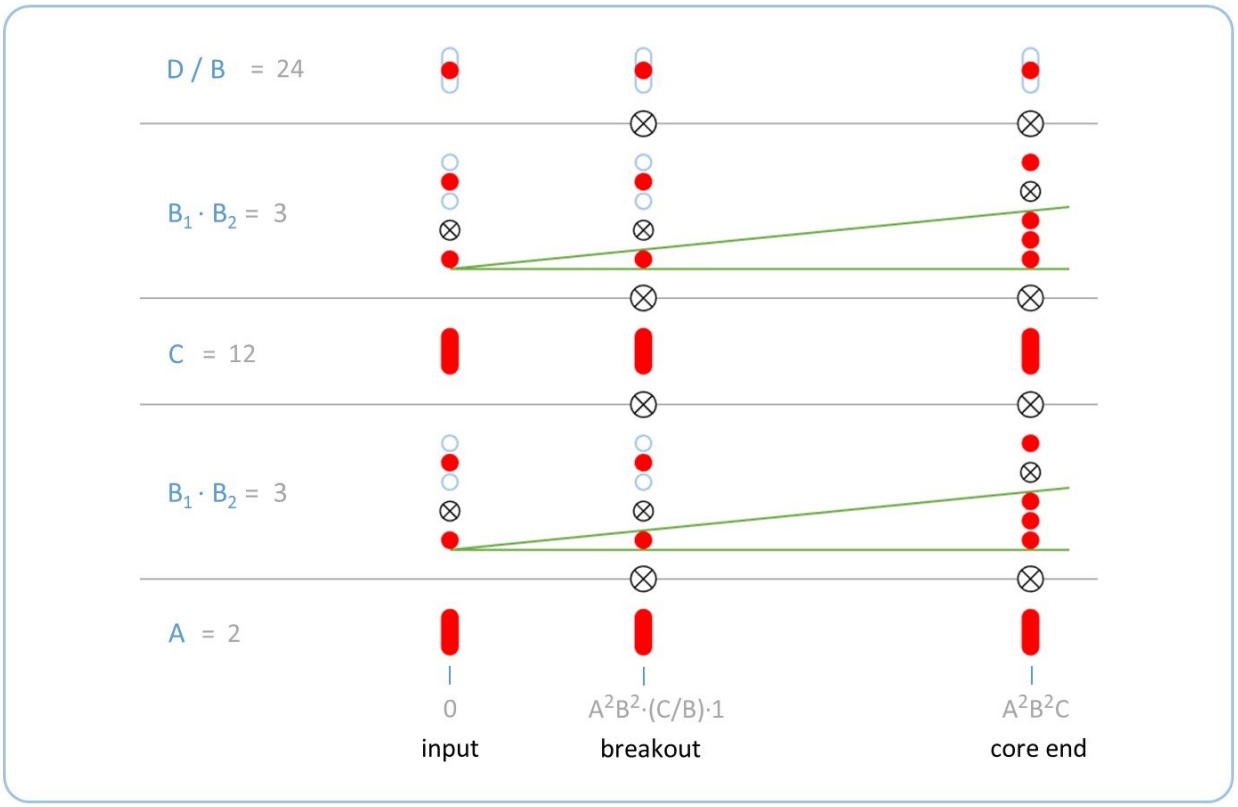

This stage is the first in which the pattern expands into the surrounding dark space, i.e. beyond the extent of the overall pattern at the start. This growth must be balanced by a shrinking of the top-ranking dark feature D. This shows that FO always must always assume a finite boundary to the space under consideration, set by the focal length of the lens. To model the unbounded propagation of light, for example in astronomy, FO would need to imagine a theoretical lens of enormous size.

9 The late elbow

At the core end, several instances of the late beam lie adjacent to one another. In this stage these instances spread apart from one another, forming the distinct diffraction orders seen in the far field, see figure 9.1.

figure 9.1, Spatial diagram of stage approaching the late elbow

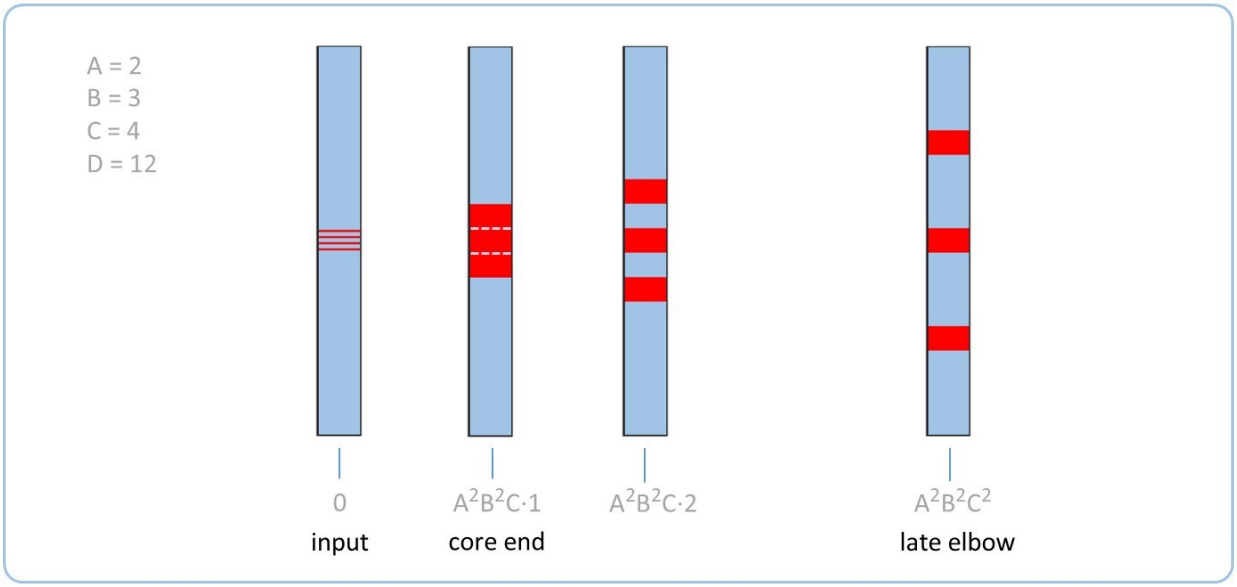

See companion code in lateElbow.m

Again we see a structural mirror symmetry between this stage and the stage leading up to the core start. However, there is an essential difference: there, the width of the overall pattern remains fixed, and an increase in bright area necessarily comes at the cost of a decrease in dark area. Here, the overall pattern area expands. As the dark area grows, the bright area becomes smaller *relative* to the dark area, but the size of beam instances actually remains constant in absolute terms.

The feature diagram in figure 9.2 contrasts with the similar growth of dark area during the early revivals. There, the growth in the dark feature is absorbed by a shrinkage of the bright feature ranking immediately above it. Here, as the dark feature grows to size C, the bright feature B directly above it 'floats' further up without shrinking. Instead, the increased pattern size is absorbed by shrinkage of the top-ranking dark feature.

figure 9.2, Feature diagram of stage approaching the late elbow

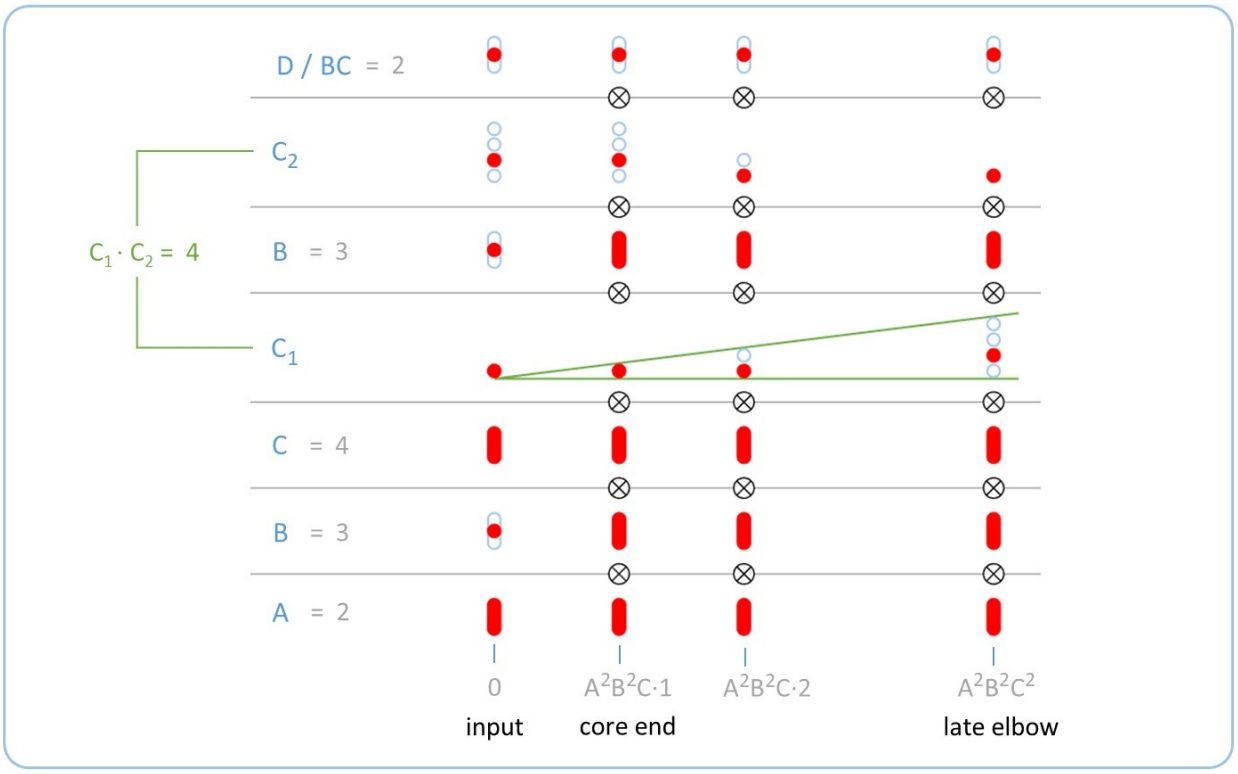

10 The end field

As discussed earlier, a beam in FO consists of two regions: a collimated region that propagates without widening, and a cone-like region that widens proportionally to distance Z. The entire course of propagation up to the late elbow can be seen as the collimated region of the late beam, with constant width ABC.

After the late elbow, the late beam begins to widen. As drawn in figure 10.1, this causes the entire pattern to widen proportionally to Z. Unlike in previous stages, the shape of the pattern does not change; rather, it grows by a simple magnification factor. All sizes in the pattern remain the same *relative* to one another.

figure 10.1, Spatial diagram of stage approaching the end field

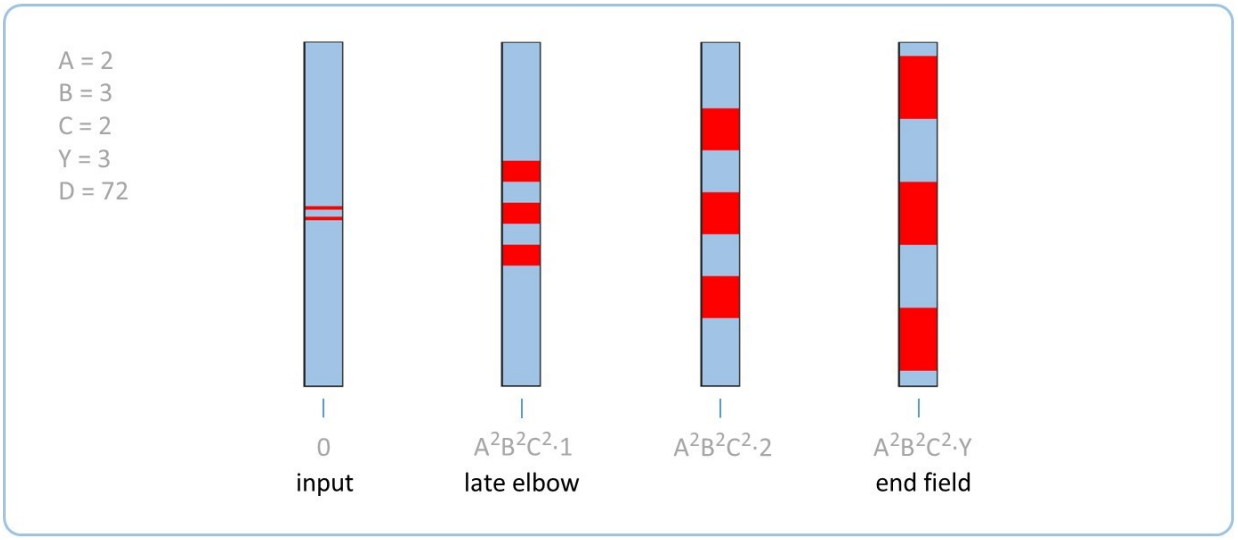

Also unlike previous stages, the length of this stage and the amount of feature growth does not depend on one of the parameters A, B, or C that define the grating. Rather, it depends on the magnification factor Y that simply represents the ratio between the Z distance of the late elbow and the lens focal length. For a greater focal length, the magnification factor Y simply increases proportionally.

Also, the Fourier transform is essentially complete by the late elbow (apart from curvature, which will not be considered until the next section). The additional magnification at the end field can be considered a physical manifestation of the rule[5] that the FT of a function that has been 'padded' or extended with extra zeros yields the FT of the original function, with new points added interstitially by bandwidth-limited interpolation.

figure 10.2, Feature diagram of stage approaching the end field

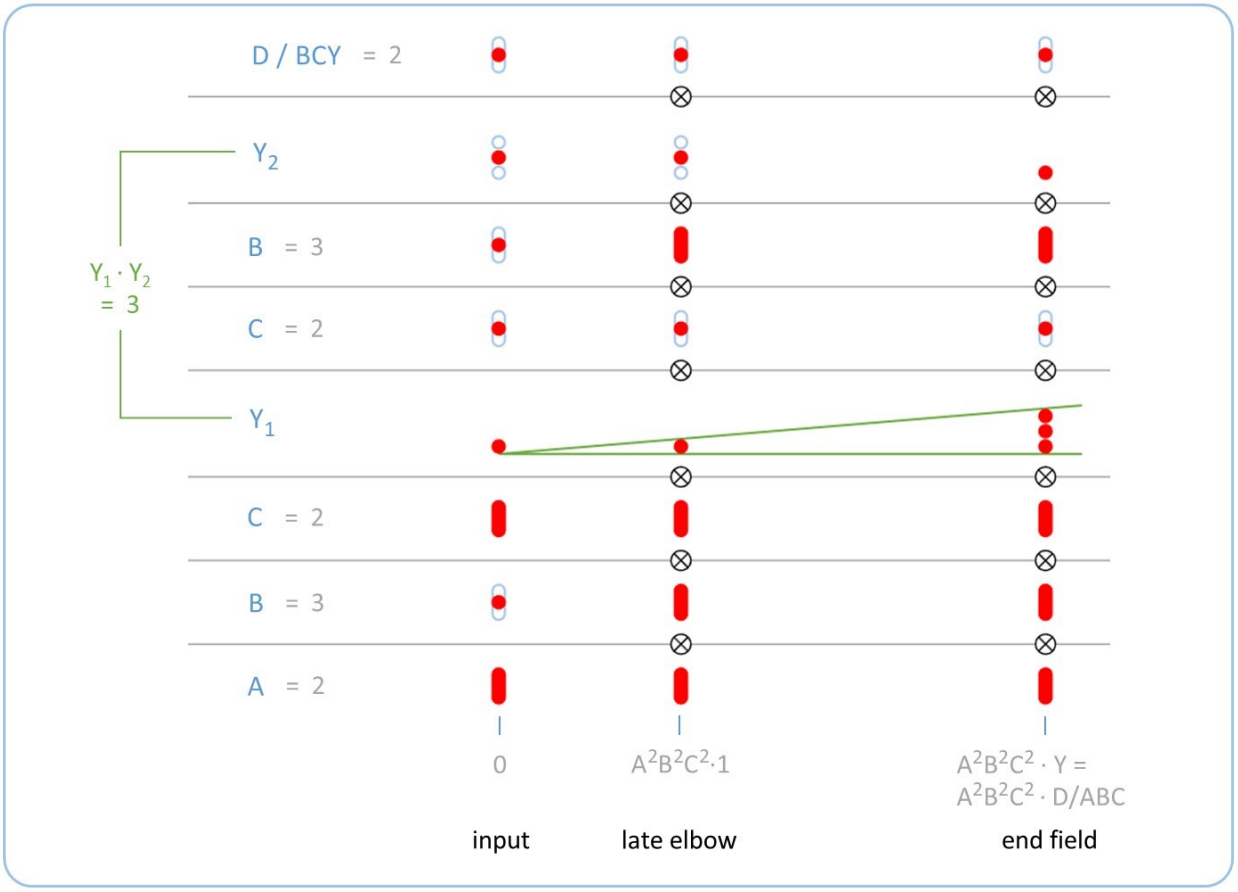

11 The lens and flip field

Immediately after the end field the light passes through the lens, which changes its curvature. The light then propagates one additional focal length through the *flip field* before reaching the rear focal plane, where the FT reaches completion.

Because the focal length is larger than the Z distance of the late elbow, the pattern of light remains constant in the flip field apart from curvature. FO does not presently describe curvature, so the spatial and feature diagrams for any plane in the flip field are simply the same as those at the end field.

The net effect of propagation between input and output planes is to perform the FT; a key result of FO is that the FT reverses the nesting rank of the features and flips each from dark to bright, or vice-versa. As shown in figure 11.1, the top-ranking dark feature of total size D at the input can be factored into four features of sizes B, C, Y, and A. The dark features B, C, and Y form the available dark space into which the light expands in the stages leading to the core end, late elbow, and end field, respectively. The dark feature A represents the available space that

remains dark because of the limited divergence of the expanding pattern. Alternatively, it can be thought of as the (inverse) f-number of the early beam.

figure 11.1, Feature diagram of input and output planes

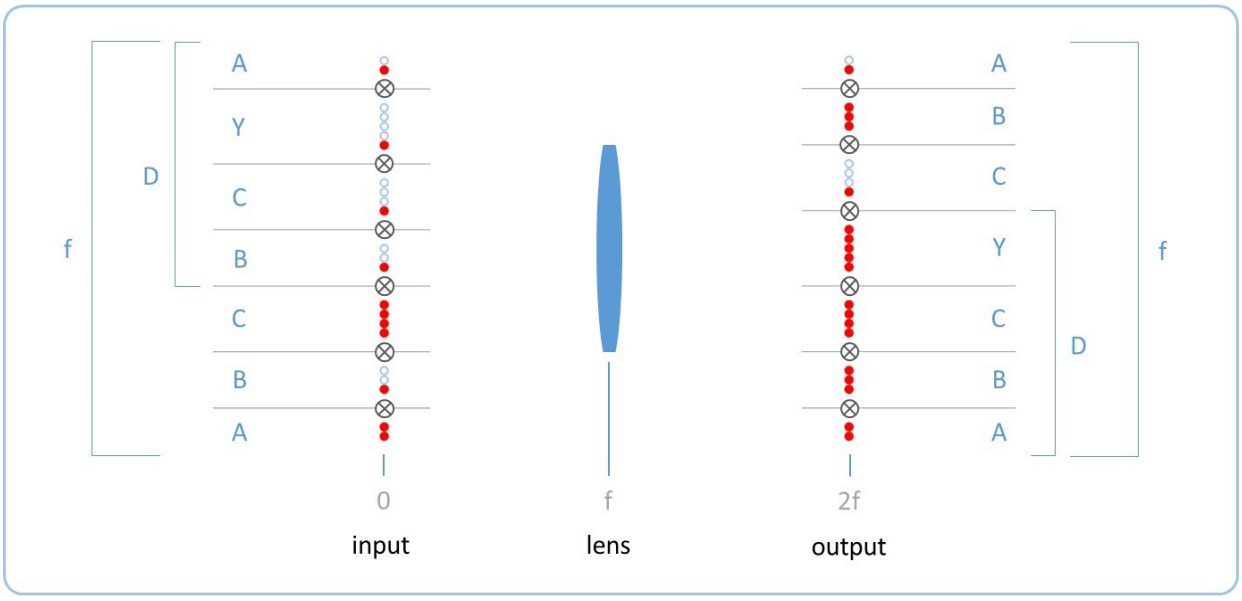

The ranking of factors A, Y, C, and B within the feature D is not physically observable. However, they are 'filled', or flipped to become bright features, from the inside out and therefore best expressed in the order shown in the figure. At the output, the order is different to reflect the structure of the output pattern.

12 Discussion

12.1 Summary diagram

We summarize our stage-by-stage analysis in figure 12.1. Note that unlike most of the figure in this work, the scale of the horizontal axis is *not* linear, but instead is approximately logarithmic.

figure 12.1, Feature diagram of all critical planes

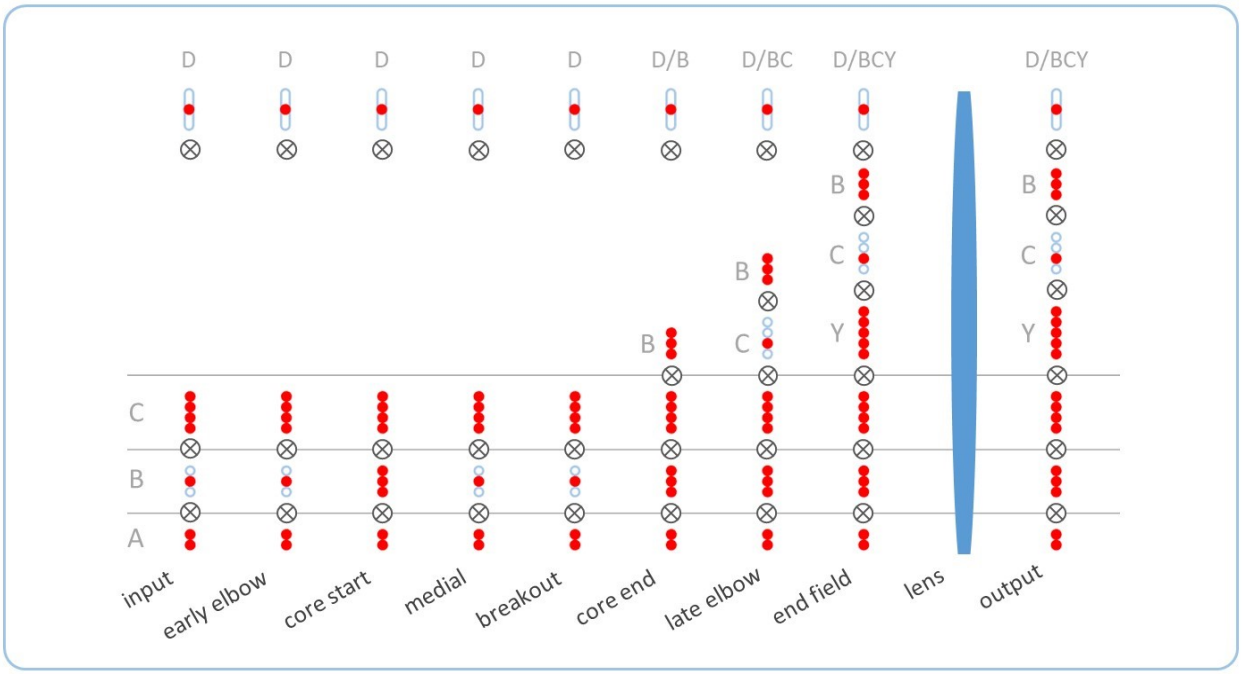

12.2 Comparing FO against the conventional model

We now turn to the conventional view of the grating, drawn in figure 12.2. Diffraction of all types of patterns – not just gratings – is conventionally divided into two main regions: the near field and the far field, also referred to as the Fresnel region and the Fraunhofer region, respectively. The boundary is not sharp, and the theories are most accurate at planes that are far away from it. It is determined by a single dimension: the overall width of the starting pattern.

figure 12.2, Conventional outline of the propagating grating

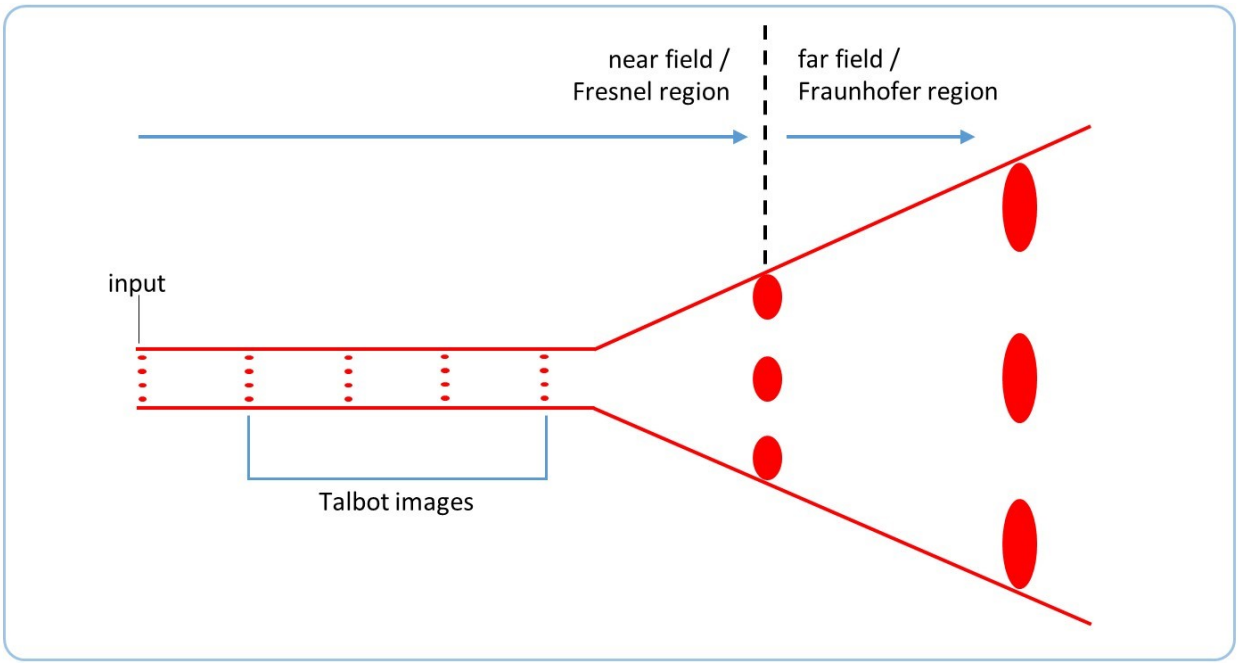

A typical pattern has just one such characteristic size, but the grating actually has 3 characteristic sizes: the early beam width, the late beam width, and the period. Each of these can be treated as the characteristic width of a beam, and each in turn defines a boundary plane – the early elbow, the late elbow, and the medial, respectively. The latest boundary plane – the late elbow – corresponds to the conventional near / far field boundary.

Within the near field lie the planes conventionally known as *Talbot images* but also referred to as *self-images* and *Fresnel images*. These occur as the light from the various source apertures blurs and interferes, forming complicated patterns that fluctuate rapidly with distance. However at certain planes the light appears to spontaneously 'de-blur' as if by magic, and re-form into the original grating pattern. In a variant, it may form an 'image' in which the period is smaller than the original.

The Talbot image at the medial is staggered laterally by half a period from the input pattern. At 2x the medial distance, the pattern is once again aligned with the starting pattern. Authors disagree about which distance to consider more fundamental; we follow Wen[6] in calling them the secondary and primary Talbot distances, respectively.

FO categorizes all of these planes differently from conventional theory, as shown in figure 12.3. Firstly, FO gives a place of special importance to the medial. It is both the last of the early revivals, and the first of the late revivals. As we will discuss later, it is also a point of structural symmetry. However in the conventional view it is merely the first of many Talbot images, and a secondary Talbot image at that.

figure 12.3, Conventional vs FO views of Talbot images / revivals

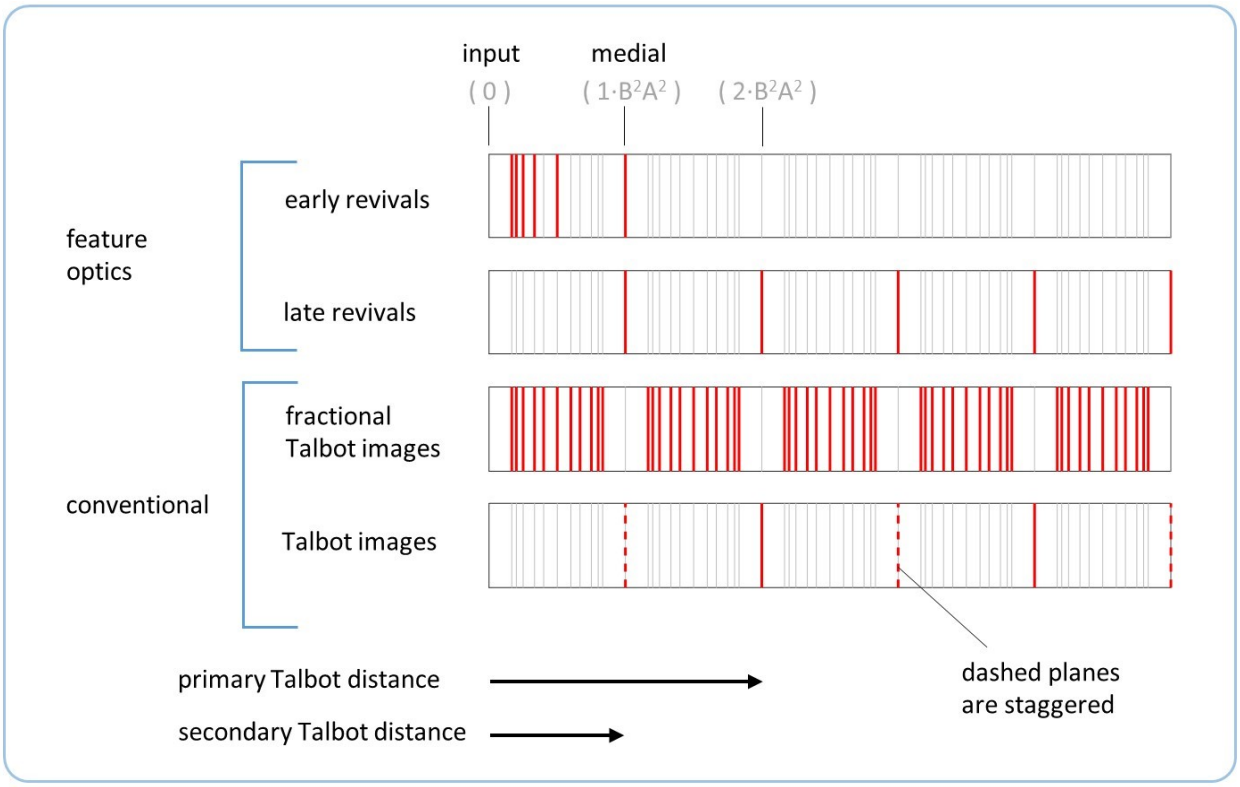

Secondly, the conventional view considers all revival-like planes in between any of the full-period planes to be *fractional* Talbot images. These are an infinite set, and occur at

$$Z = \frac{p}{q} \cdot \frac{d^2}{\lambda}$$

Where d is the period of the grating, and p and q are all possible coprime integers[6]. However, FO treats only the cases in which p = 1 and q < B, in which case the foregoing equation is equivalent to that shown in section 6 as the condition for early revivals. This includes only some of the fractional Talbot images before the medial, and none after the medial. It is a matter for future research to determine whether FO can be expanded to account for all the revival-like planes which it currently neglects.

12.3 Longitudinal nesting

An individual plane in FO has a nested structure – for instance, an bright feature nested under a dark feature, all nested under an bright feature, etc. This pattern lies in a plane *transverse* to the propagation.

Over the course of many stages, we also observe that the critical planes themselves appear to be *longitudinally* nested in Z, each within the next. This is most easily seen in the table in figure

12.4. Each stage follows the same recursive formula: it begins at some distance, and ends at a new distance that is greater by some *increase factor*. The end of one stage marks the beginning of the next, etc.

figure 12.4, Longitudinally nested planes

plane	increase factor	Z
end field	Y	$A^2 \cdot B^2 \cdot C^2 \cdot Y$
late elbow	C	$A^2 \cdot B^2 \cdot C^2$
core end	C	$A^2 \cdot B^2 \cdot C$
breakout		$A^2 \cdot B^2 \cdot (C/B)$
medial	B	$A^2 \cdot B^2$
core start	B	$A^2 \cdot B$
early elbow	A	A^2
waistlength	A	A
1st wave	-	1

The increase factors follow a simple progression: they begin with the size of the lowest-ranking feature in the starting pattern (size A), and proceed upwards. For each starting feature, *two* increase factors are applied sequentially.

In many but not all stages, a new feature seems to grow in the chain of features. When this occurs, the size of the new feature also matches the increase factor for that stage.

While this trend can be traced backwards all the way to the first wave (Z = 1), it can never reach Z = 0 by dividing by any finite factors. This is surprising, because the pattern before the early elbow looks identical to the input pattern, and they appear as though they are connected by a continuous trend.

12.4 Rough symmetry

The medial is a plane of rough *structural mirror symmetry* along the direction of propagation. The table in figure 12.5 shows that for (nearly) each critical plane *before* the medial, there is a corresponding critical plane *after* the medial which is its 'mirror partner'. The medial plays the role of the 'mirror' itself, which is the source of its name.

figure 12.5, Mirror symmetries

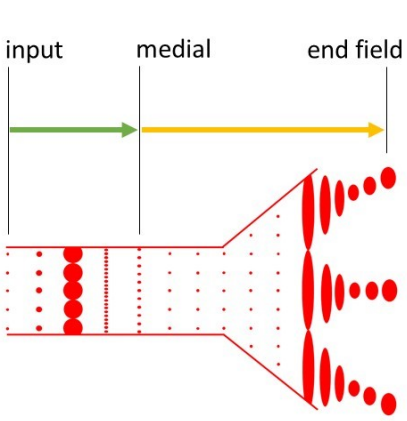

early	late
waistlength	end field
early elbow	late elbow
core start	core end
early revivals	late revivals
---	breakout
medial	medial

Note that the system is *not* symmetric in the ordinary, spatial sense. For instance, the early elbow has C instances of a small beam, but its mirror partner is the late elbow which has B instances of a large beam. However, there is nevertheless a symmetry to the logic of how transitions occur from one region to another. Any principle or statement regarding one critical plane usually applies in some analogous way to its mirror partner.

The logical symmetry is imperfect in some respects. For instance, early revivals taken as a whole occupy a symmetrical role to the late revivals, taken as a whole. However, it is not possible to match each individual early revival with a corresponding late revival, because there are B early revivals and (C/B) late revivals.

There exists one strong asymmetry: the breakout has no corresponding plane before the step. This is a consequence of the fact that we are considering the *late-breaking grating* case in which C > B and the breakout occurs after the medial.

13 Conclusion

As in previous work, we have shown that FO provides a curiously appropriate system for describing the diffraction grating. Stated another way, we have shown how all the patterns emerging from the grating appear to be confined to the rather narrow parameter space that FO affords. This suggests (though it does not yet prove) that FO may offer a window into deeper insights into the grating.

It is surprising that FO works as well as it does, considering that it bears no obvious resemblance to any existing theory of optics. Our present conception of the electromagnetic field is defined

by Maxwell's equations, which deal with continuous fields varying across space, along with their derivatives. The nested patterns in FO instead suggest a strange hierarchical structure of space.

This work has treated the diffraction grating at the level of description, rather than explanation. We have not attempted to interpret FO in terms of wave optics or any other theory. We have also not proposed any laws or mechanisms by which features evolve, nor any other reason why the critical planes have the form that they do.

14 References

1. Mirsky, Paul L. A First Look at Feature Optics. http://vixra.org/abs/1909.0157, 2019

2. Github repository at https://github.com/paulmirsky/criticalPlanes

3. Berry, M.V. and Klein, S. Integer, fractional, and fractal Talbot effects. Journal of Modern Optics, 1996, vol 43, no. 10, 2139-2164

4. Berry, Michael; Marzoli, Irene; and Schleich, Wolfgang. Quantum carpets, carpets of light. Physics world, June 2001

5. Smith, Julius O., III. Mathematics of the Discrete Fourier Transform (DFT) with Audio Applications, 2nd edition. See https://www.dsprelated.com/freebooks/mdft/

6. Wen, J., Zhang, Y., and Xiao, M. The Talbot effect: recent advances in classical optics, nonlinear optics, and quantum optics. Adv Opt Photonics 5, 83–130, 2013